Available online at www.sciencedirect.com
ScienceDirect
Scripta Materialia 61 (2009) 967–969
Scripta MATERIALIA
www.elsevier.com/locate/scriptamat

Structural changes induced by microalloying in $Cu_{46}Zr_{47-x}Al_7Gd_x$ metallic glasses

Xue-Kui Xi,[a] Magdalena Traico Sandor,[a] Yan-Hui Liu,[b] Wei-Hua Wang[b] and Yue Wu[a,*]

[a]*Department of Physics and Astronomy, University of North Carolina, Chapel Hill, NC 27599-3255, USA*
[b]*Institute of Physics, Chinese Academy of Sciences, Beijing 100190, China*

Received 26 May 2009; accepted 3 August 2009
Available online 7 August 2009

^{27}Al nuclear magnetic resonance spectroscopy was used to probe the atomic-scale structural evolution in $Cu_{46}Zr_{47-x}Al_7Gd_x$ ($x = 0$, 1, 5) glassy alloys with minor Gd addition. It was found that the local symmetry of atomic clusters around Al atoms is the closest to being spherical at 1 at.% Gd addition. Interestingly, this also corresponds to the Gd content for which the glass-forming ability (GFA) reaches a maximum, suggesting that the GFA of these glassy alloys may be dominated by their local geometric structure.

Keywords: Metallic glasses; Nuclear magnetic resonance (NMR); Short-range order (SRO)

The discovery of bulk metallic glasses (BMGs) with unique mechanical and functional properties has inspired intensive research on the local structures of metallic glasses as well as the structural origin of the microalloying effects of glass-forming ability (GFA) and mechanical properties [1–3]. Short-range order and medium-range order have long been considered to be important for understanding the properties of amorphous solids including metallic glasses [4–7]. However, it remains a very challenging task to characterize these local structures experimentally because of the complexity and disordered nature of glassy structures [8]. CuZrAl BMGs are very interesting because of their high GFA and unusual plasticity [9–11]. Furthermore, minor Gd addition was found to induce an obvious ductile-to-brittle transition along with a substantial change in GFA [12–14]. This paper describes evidence of significant structural changes in CuZrAl BMGs upon minor Gd addition detected by ^{27}Al nuclear magnetic resonance (NMR) spectroscopy. NMR measurements of quadrupole interactions have been used extensively to characterize local structures in amorphous solids [15–17]. Such measurement probes the electric-field-gradient (EFG) at the atom of interest, such as Al in CuZrAl BMGs, and depends sensitively on the local structure around that atom. It was found that the magnitude of the EFG at Al sites in CuZrAl BMG decreases first with minor Gd addition, reaching a minimum at 1 at.% Gd and then increases again at 5 at.% Gd. This change in EFG correlates with the change in macroscopic properties such as the GFA. When the GFA reaches its maximum, the EFG at Al sites reaches a minimum.

$Cu_{46}Zr_{47-x}Al_7Gd_x$ ($x = 0$, 1, 5) metallic glass cylinders 2 mm in diameter were prepared by a conventional copper mold casting method [13]. ^{27}Al nutation NMR was performed in a magnetic field of 7.01 T. The pulse sequence used is $(t_1)_x$–τ_1–$(t_2)_x$–τ_2–acquisition$_{-y}$, where t_1 and t_2 are radiofrequency (RF) pulse widths, x and $-y$ are pulse and receiver phases, respectively, and τ_1 and τ_2 are time delays. The RF pulse strength employed is $\omega_{rf}/2\pi = 50$ kHz, $t_1 = 1$ μs, $\tau_1 = 10$ μs, and the echo signal appearing at $\tau_2 = \tau_1$ was recorded. The signal intensity associated with the central transition $|-1/2\rangle \leftrightarrow |1/2\rangle$ was then determined as a function of t_2, called the nutation curve, in a series of measurements where t_2 varies from 1 to 7 μs in steps of 0.5 μs. The EFG parameters were derived from numerical simulation of the nutation curve. For comparison, the ^{27}Al spectra were also measured by point-by-point mapping using weak selective pulses. ^{27}Al Knight shifts were referenced to 1.0 M $Al(NO_3)_3$ aqueous solution.

Figure 1 shows the nutation curves for all three $Cu_{46}Zr_{47-x}Al_7Gd_x$ ($x = 0$, 1, 5) BMG samples; there are clear differences between the curves. The nutation curve is determined by the applied RF field ω_{rf} and

* Corresponding author; E-mail: yuewu@physics.unc.edu

1359-6462/$ - see front matter © 2009 Acta Materialia Inc. Published by Elsevier Ltd. All rights reserved.
doi:10.1016/j.scriptamat.2009.08.002

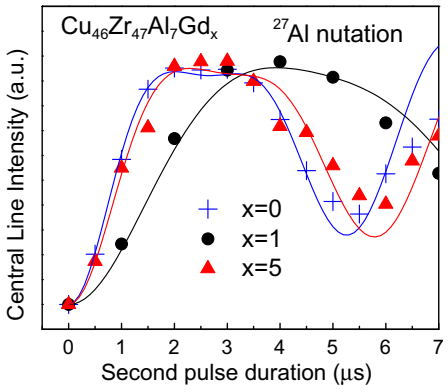

Figure 1. Nutation experiments where the central transition intensity is plotted vs. the second pulse length. The pulse length t_2 increases from 0 to 7 μs in steps of 0.5 μs. The amplitude of the RF pulse is $\omega_{rf}/2\pi = 50$ kHz for all three samples. Solid lines are fittings with $\omega_Q/2\pi$ listed in Table 1 and $\eta = 0.9$ as described in the text.

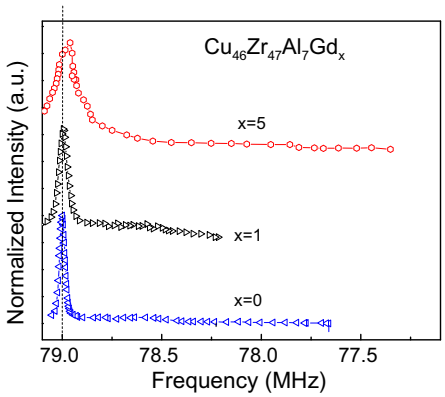

Figure 2. ^{27}Al spectra (partial) of $Cu_{46}Zr_{47-x}Al_7Gd_x$ ($x = 0$, 1, 5) BMGs obtained by the frequency stepped point-by-point method. The linewidth of the satellite transitions can be estimated by the extension of the lines. The intensity is normalized by peak intensity.

the quadrupole interaction determined by $\omega_Q = 3Qe^2q/[2I(2I-1)\hbar]$ and η [15]. Here, ω_Q is the quadrupole frequency, Q is the electric quadrupole moment, $eq = V_{ZZ}$ is the Z principal component of the EFG tensor which vanishes under cubic or higher symmetries, $I = 5/2$ for ^{27}Al, and η is the asymmetry parameter of the EFG tensor. Given the ratio of ω_{rf}/ω_Q, and η, the nutation curve can be calculated based on the evolution of the density operator. The best fits of the calculated nutation curves to the measured ones were also shown in Figure 1. Here, $\eta = 0.9$ was used for all three curves and the values of the quadrupole frequency $\omega_Q/2\pi$ are listed in Table 1. Clearly, $\omega_Q/2\pi$ changes with the minor addition of Gd. It decreases significantly from 650 kHz in the $x = 0$ sample to 450 kHz in the $x = 1$ sample. This implies that the degree of local site symmetry at Al nuclei is enhanced when adding 1 at.% Gd. Interestingly, $\omega_Q/2\pi$ increases again to 600 kHz in the $x = 5$ sample.

Figure 2 shows the point-by-point mapped ^{27}Al spectra of $Cu_{46}Zr_{47-x}Al_7Gd_x$ BMGs with $x = 0$, 1 and 5 at room temperature. The spectra have a broad peak and a sharp peak, which originate from the satellite transitions and the central transition, respectively. It is worth noting here that the primary ^{27}Al spectral satellite linebroadening mechanisms in this alloy system might be ascribed to the following: (i) first-order quadruple perturbation through EFG; and (ii) the broadening effects of the localized 4f electron magnetic moment of Gd^{3+} ions [18]. Since the central linewidth for all the samples investigated are symmetric for 30 ($x = 0$) to 300 kHz ($x = 5$), at least one order of magnitude less than that of satellite linewidth and field independent, indicating the Gd^{3+} magnetic moment effects on satellite line broadening can be neglected. The linewidth of the broad peak associated with the satellite transitions is thus determined by the first-order quadrupole interaction and can also be used to estimate the quadrupole frequency $\omega_Q/2\pi$ [17]. The broad peak of the satellite transitions spans a range of 2.68 MHz at $x = 0$, narrows to 1.54 MHz at $x = 1$, and then broadens again to 3.30 MHz at $x = 5$. The $\omega_Q/2\pi$ values determined from the linewidth of the satellite transitions are also listed in Table 1 and are consistent with the nutation measurements.

Figure 3 shows the correlation of quadrupole frequency with macroscopic properties such as GFA. It can be seen that the increase in critical diameter D_c, which has been widely used as a convenient and reliable method to evaluate GFA, correlates very well with the decrease in the quadrupole frequency and is consistent with previous observations in Ce-based BMGs [7]. These results suggest that GFA is favored by the evolution of the atomic structure at Al sites toward higher local symmetry with lower local strains [19].

It is interesting to note that different amorphous phases with the same composition but different densities have been observed in amorphous solids that form network structures [20]. For metallic glasses, this is also an important issue of current interest. Evidence of pressure-induced polyamorphic transition has been reported in Ce-based metallic glass [21]. This phenomenon could be related to the unique electronic properties of Ce atoms which can assume different valencies under pressure as observed in Ce metal [22,23]. The microalloying effect in BMGs provides another approach for studying

Table 1. Room temperature (298 K) ^{27}Al isotropic peak shifts, satellite linewidth, quadrupole frequency measured via linewidth analysis and nutation methods, respectively, GFA evaluated in critical diameter, and plastic strain of $Cu_{46}Zr_{47-x}Al_7Gd_x$.

$Cu_{46}Zr_{47-x}Al_7Gd_x$	Peak shift (ppm)	Satellite linewidth (MHz)	Quadruple frequency (kHz) (linewidth)	Quadruple frequency (kHz) (nutation)	Critical diameter (D_c, mm)	Plastic strain[a] (%)
$x = 0$	300	2.68	670	650	3	3.20
$x = 1$	295	1.54	385	450	10	3.75
$x = 5$	0	3.30	825	600	5	1.98

[a] Ref. [14].

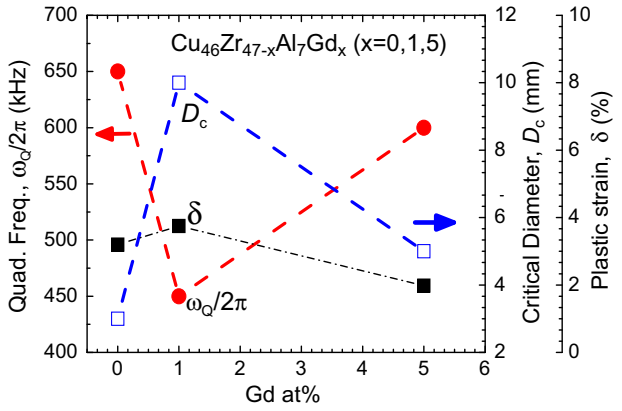

Figure 3. Critical diameter (D_c) [13], plastic strain (%) [14] and measured quadrupole frequency $\nu_Q = \omega_Q/2\pi$ are plotted vs. the Gd concentration. It shows a clear correlation between the GFA and $\omega_Q/2\pi$.

polyamorphism because there is no substantial change of composition while there is a clear change in local structure. The structural change induced by 1 at.% Gd addition in CuZrAl BMG could be such an example (see Fig. 3). It is intriguing that 1 at.% Gd addition leads to such significant evolution in the amorphous inherent structure, which is reminiscent of similar effects of microalloying in crystalline systems such as the addition of C in steel or Al in Ti alloy. The addition of 1 at.% C stabilizes austenite phase (face-centered cubic) in steels; 2 at.% Al addition promotes the formation of the α phase (hexagonal close packed) in Ti alloys [24]. From the point of view of the energy landscape, glass structures could assume various metastable inherent structures upon cooling of the supercooled liquid, $A_1, A_2, \ldots, A_n$. Are there distinct structural characteristics of these inherent structures? It is conceivable that 1 at.% Gd addition might favor one of the inherent structures with high local symmetry at Al sites over other possible inherent structures in CuZrAl BMGs. The current NMR results indicate that microalloying is a viable approach for exploring different inherent structures with distinct local structures.

We have no data on the parameters of quadrupole interaction for compositions between 2 and 4 at.% Gd. Verification on the correlation of the improved local symmetry at Al sites and enhanced GFA is thus incomplete. However, our results demonstrate that minor addition of Gd in CuZrAl BMGs induces significant changes in local structures. Such changes can be detected by NMR through the detection of the change in the EFG at Al sites. A clear correlation is found between the GFA and the characteristics of the local structure. Specifically, the composition of CuZrAl(Gd) with the highest GFA corresponds to local structures closest to spherical symmetry at Al sites.

This work was supported by the US Army Research Office (Grant No. W911NF-09-1-0343), National Science Foundation of China (Grant No. 50621061) and Chinese Academy of Sciences.

[1] W.L. Johnson, MRS Bull. 24 (1999) 42.
[2] A. Inoue, Acta Mater. 48 (279) (2000).
[3] A. Sadoc, M. Sabra, O. Proux, J.L. Hazemann, K.S. Bondi, K.F. Kelton, Philos. Mag. 88 (2008) 2569.
[4] T. Egami, Y. Waseda, J. Non-Cryst. Solids 64 (1984) 113.
[5] D.B. Miracle, W.S. Sanders, O.N. Senkov, Philos. Mag. 83 (2003) 2409.
[6] Y. Zhang, A.L. Greer, Appl. Phys. Lett. 89 (2006) 71907.
[7] X.K. Xi, L.L. Li, B. Zhang, W.H. Wang, Y. Wu, Phys. Rev. Lett. 99 (2007) 095501.
[8] H.W. Sheng, Y.Q. Chen, P.L. Lee, S.D. Shastri, E. Ma, Acta Mater. 56 (2008) 6264.
[9] J. Eckert, J. Das, S. Pauly, C. Duhamel, K.B. Kim, S. Yi, W.H. Wang, Mater. Trans. JIM 48 (2007) 1806.
[10] G. Kumar, T. Ohkubo, T. Mukai, K. Hono, Scr. Mater. 57 (2007) 173.
[11] L.Y. Chen, Z.D. Fu, G.Q. Zhang, X.P. Hao, Q.K. Jiang, X.D. Wang, Q.P. Cao, H. Franz, Y.G. Liu, H.S. Xie, S.L. Zhang, B.Y. Wang, Y.W. Zeng, J.Z. Jiang, Phys. Rev. Lett. 100 (2008) 075501.
[12] D.H. Xu, G. Duan, W.L. Johnson, Phys. Rev. Lett. 92 (2004) 245504.
[13] P. Yu, H.Y. Bai, W.H. Wang, J. Mater. Res. 21 (2006) 1674.
[14] E.S. Park, J.S. Kyeong, D.H. Kim, Scr. Mater. 57 (2007) 49.
[15] P.P. Man, Solid State Nucl. Magn. Reson. 2 (1993) 165.
[16] D. Freude, J. Haase, in: P. Diehl, E. Fluck, H. Günther, R. Kosfeld, J. Seelig (Eds.), NMR Basic Principles and Progress, vol. 29, Springer-Verlag, Berlin, 1993, pp. 1–90.
[17] H. Eckert, Prog. Nucl. Magn. Reson. Spectrosc. 24 (1992) 159.
[18] C.P. Grey, N. Dupre, Chem. Rev. 104 (2004) 4493.
[19] T. Egami, Mater. Sci. Eng. A 226–228 (1997) 261.
[20] O. Mishima, H.E. Stanley, Nature 396 (1998) 329.
[21] H.W. Sheng, H.Z. Liu, Y.Q. Cheng, J. Wen, P.L. Lee, W.K. Luo, S.D. Shastri, E. Ma, Nat. Mater. 6 (2007) 192.
[22] Q.S. Zeng, Y.C. Li, C.M. Feng, P. Liermann, M. Somayazulu, G.Y. Shen, H.K. Mao, R. Yang, J. Liu, T.D. Hu, J.Z. Jiang, Proc. Natl. Acad. Sci. USA 104 (2007) 13565.
[23] J.M. Lawrence, P.S. Riseborough, R.D. Parks, Rep. Prog. Phys. 44 (1981) 1.
[24] T.B. Massalski, H. Okamoto (Eds.), Binary Alloy Phase Diagrams, second ed., ASM International, Materials Park OH, 1990.